Association of Calnexin with Wild Type and Mutant AVPR2 that Cause Nephrogenic Diabetes Insipidus†

Jean-Pierre Morello,‡,§ Ali Salahpour,‡ Ulla E. Petäjä-Repo,‡,$,¶ André Laperrière,‡ Michèle Lonergan,§ Marie-Françoise Arthus,§ Ivan R. Nabi,# Daniel G. Bichet,§ and Michel Bouvier*,‡,§

Département de biochimie and Le groupe de recherche sur le système nerveux autonome, Université de Montréal, Montréal, Quebec, Canada, Unité de recherche clinique, Centre de recherche et Service de néphrologie, Hôpital du Sacré-Coeur de Montréal, Montréal, Québec, H4J 1C5, Canada, and Département de médecine, and Département de pathologie et biologie cellulaire, Université de Montréal, Montréal, Québec, H3C 3J7, Canada, and AstraZeneca R&D Montreal, St. Laurent, Quebec H4S1Z9, Canada

Received November 27, 2000; Revised Manuscript Received March 29, 2001

ABSTRACT: Over 155 mutations within the V2 vasopressin receptor (AVPR2) gene are responsible for nephrogenic diabetes insipidus (NDI). The expression and subcellular distribution of four of these was investigated in transfected cells. These include a point mutation in the seventh transmembrane domain (S315R), a frameshift mutation in the third intracellular loop (804delG), and two nonsense mutations that code for AVPR2 truncated within the first cytoplasmic loop (W71X) and in the proximal portion of the carboxyl tail (R337X). RT-PCR revealed that mRNA was produced for all mutant receptor constructs. However, no receptor protein, as assessed by Western blot analysis, was detected for 804delG. The S315R was properly processed through the Golgi and targeted to the plasma membrane but lacked any detectable AVP binding or signaling. Thus, this mutation induces a conformational change that is compatible with endoplasmic reticulum (ER) export but dramatically affects hormone recognition. In contrast, the W71X and R337X AVPR2 were retained inside the cell as determined by immunofluorescence. Confocal microscopy revealed that they were both retained in the ER. To determine if calnexin could be involved, its interaction with the AVPR2 was assessed. Sequential coimmunoprecipitation demonstrated that calnexin associated with the precursor forms of both wild-type (WT) and mutant receptors in agreement with its general role in protein folding. Moreover, its association with the ER-retained R337X mutant was found to be longer than with the WT receptor suggesting that this molecular chaperone also plays a role in quality control and ER retention of misfolded G protein-coupled receptors.

Proper water homeostasis is maintained, in part, by the action of the antidiuretic hormone arginine vasopressin (AVP)[1] on the collecting tubules of the kidney. The principal cells of the collecting tubule are polarized into an apical surface that faces the lumen of the collecting duct and a basolateral surface that faces the blood circulation. Upon release from the posterior pituitary, AVP mediates its antidiuretic action by binding to the V2 vasopressin receptor (AVPR2) (*1*), which is located on the basolateral surface of the principal cells. The AVPR2 is a member of the large family of G protein-coupled receptors (GPCR) that is coupled to the stimulatory G protein (Gs) and, when stimulated with AVP, raises the intracellular cAMP concentration by activating adenylyl cyclase. Ultimately, this leads to the insertion of aquaporin-2 water channels (*2*) into the apical membrane of the principal cell thus allowing the re-uptake of water (*3*).

Inactivating mutations in the gene coding for the AVPR2 are responsible for an X-linked hereditary disease known as nephrogenic diabetes insipidus (NDI) (*3*). Over 150 different mutations in this gene have been reported to date and of these, over 79 have been expressed in heterologous expression systems (*4*−*25*). Surprisingly, over 70% of the expressed mutations lead to receptor proteins that are not expressed on the cell surface. Although in rare cases, this may result from the lack of synthesis of a stable protein (*11*), it is

† J.P.M. held a studentship from the Medical Research Council of Canada (MRCC)/PMAC Health Program. A.S. is supported by a studentship from the MRCC. M.B. is an MRCC Scientist. This work was supported by grants from the Kidney Foundation of Canada (D.G.B., M.B.), from the MRCC (D.G.B., M.B., I.R.N.), and from la Fondation J. Rodolphe-La Haye (D.G.B.)

* To whom correspondence should be addressed at the Université de Montréal, Département de biochimie, Faculté de Médecine, P.O. Box 6128, Downtown station, Montreal, Qc H3C 3J7, Canada. Phone: (514) 343-6372. Fax: (514) 343-2210. E-mail: bouvier@bcm.umontreal.ca.

‡ Département de biochimie and Le groupe de recherche sur le système nerveux autonome, Université de Montréal.

§ Hôpital du Sacré-Coeur de Montréal.

Département de pathologie et biologie cellulaire, Université de Montréal.

$ AstraZeneca R&D Montreal.

¶ Present address: Department of Anatomy and Cell Biology, University of Oulu, P.O. Box 5000, FIN-90014 Oulu, Finland.

[1] Abbreviations: AVP, arginine-vasopressin; AVPR2, V2 vasopressin receptor; cAMP, cyclic adenosine monophosphate; cDNA, complementary DNA; DMEM, Dulbecco's modified Eagle medium; FACS, fluorescence-assisted cell sorting; ER, endoplasmic reticulum; GPCR, G protein-coupled receptor; NDI, nephrogenic diabetes insipidus; PBS, phosphate-buffered saline; PCR, polymerase chain reaction; PFA, paraformaldehyde; RT-PCR, reverse-transcription-PCR; SDS−PAGE, sodium dodecyl sulfide−polyacrylamide gel electrophoresis; WT, wild-type.

10.1021/bi002699r CCC: $20.00
Published on Web 05/12/2001

believed that in most instances the mutant receptors are being synthesized and retained intracellularly. However, specific retention in a given organelle has been documented for only a small subset.

Intracellular retention of mutant proteins has often been linked to prolonged interactions with molecular chaperones in the endoplasmic reticulum (ER) (for a review, see ref *26*). For several proteins, calnexin has been identified as one of the molecular chaperone involved (*27*−*30*). Since calnexin has previously been reported to interact with GPCRs (*31*), we sought to determine if it could be one of the chaperones involved in the intracellular retention of NDI-linked AVPR2 mutants. For this purpose, the subcellular localization of four distinct NDI AVPR2 mutants was assessed, and their propensity to interact with calnexin was determined by co-immunoprecipitation. Here we report that both wild type (WT) and mutant receptors interact with calnexin. However, ER retention was found to be associated with a longer interaction time between the mutant AVPR2 and the molecular chaperone suggesting that calnexin could play a role in the intracellular retention of misfolded GPCRs. To our knowledge, this is the first demonstration of an extended interaction between calnexin and a GPCR mutant.

EXPERIMENTAL PROCEDURES

Genomic DNA Amplification and Construction of Expression Vectors. Genomic AVPR2 DNA was amplified from NDI patients and unaffected related individuals using the polymerase chain reaction (PCR) with a mutant 27-mer oligonucleotide primer bearing a *Kpn* I site (5′-CCCAGCCCCAGGTACCTCATGTCC-3′) and a mutant 22-mer oligonucleotide primer bearing a *Sal* I site (5′-GGATCCAAGTCGACCCCTTGCC-3′), which hybridize in the 5′ and 3′ untranslated regions of this gene, respectively. The PCR fragments were digested and subcloned 3′ to the myc epitope tag sequence (MEQKLISEEDLNA) into the pBC12BI mammalian expression vector (*32*). All constructs were verified by sequencing to confirm the presence of each mutation.

Cell Culture and Transfection. COS-1 cells were transiently transfected using the DEAE-dextran method (*32*), and the cells were allowed to express the foreign DNA 48 h before performing experiments. HEK-293 cells were rendered stable for the expression of WT or R337X AVPR2 by transfection with 15 μg of receptor plasmid and 1 μg of pSV2neo (Clonetech). The cells were then passaged by serial dilution and single isolate clones were grown and maintained in Dulbecco's modified Eagle medium (DMEM) containing 10% (v/v) fetal calf serum, 1000 U/mL penicillin, 1 mg/mL streptomycin, and 300 μg/mL Geneticin (Life Technologies).

Preparation of Total mRNA and cDNA. Forty-eight hours after transfection, the culture media was removed and COS-1 cells were incubated with Trizol (Life Technologies). Total cellular mRNA was prepared following a chloroform extraction. Contaminating genomic DNA was digested with DNAse I (Life Technologies). The complete digestion of genomic AVPR2 DNA (from the transfected plasmid) was confirmed by PCR using the following primers: 5′-CCCAGCCTGCCCAGCAAC-3′ and 5′-TCCCTCTTTCCTGCCACTCCT-3′. These primers hybridize to the second exon and the 3′ untranslated region, respectively. cDNA was prepared by reverse transcription (RT)-PCR (oligo dT, Superscript, Life Technologies). The presence of AVPR2 cDNA was verified by PCR (same primers as above) by comparing the lengths of the obtained fragments (cDNA of 1361 bp versus genomic DNA of 1468 bp). In addition, the absence of *Sph* I digestion (unique site in intron 2) in the DNA fragments confirm their cDNA origin. All cDNAs were subsequently sequenced to confirm each mutation (Sequenase version 2.0 DNA sequencing kit, USB).

Western Blotting. Forty-eight hours after transfection, crude membranes from COS-1 cells were prepared by lysing the cells in buffer A (25 mM Tris-HCl, 2 mM EDTA, pH 8.0) containing the following protease inhibitors: 10 μg/mL benzamidine, 5 μg/mL leupeptin, and 5 μg/mL soybean trypsin inhibitor (all from Sigma). Cells lysates were further homogenized with a Polytron (3 times 15 s) and cleared of nuclei and unbroken cells by centrifugation at 500*g* for 10 min. The supernatant was subjected to 45000*g* for 20 min, the crude membrane pellet was washed in buffer A and recentrifuged. The total protein concentration of each sample was determined by Bradford assay (BioRad) and samples containing 100 μg of total protein were either subjected to glycine or tricine (*33*) sodium dodecyl sulfide−polyacrylamide gel electrophoresis (SDS−PAGE) and transferred to nitrocellulose (Schleider & Schuell). The nitrocellulose was blocked in phosphate-buffered saline (PBS) containing 5% milk, incubated with anti-myc antibody (9E10 from ascites fluid) followed by horseradish peroxidase-conjugated sheep anti-mouse $F(ab')_2$ fragment (Amersham Pharmacia) and revealed by chemiluminescence (Renaissance kit, NEN Life Sciences Products).

Metabolic Labeling and Immunoprecipitation. COS-1 (Figure 7) or HEK-293 (Figure 8) cells expressing the WT or mutant AVPR2 were starved for 30 min in methionine and cysteine-free DMEM and labeled with 150 μCi/mL of [^{35}S]-methionine/cysteine (EXPRE^{35}S^{35}S protein labeling mix; NEN Life Science Products) in the same medium. After an incubation of 30 (Figure 7) or 60 (Figure 8) min at 37 °C, the pulse was terminated by washing the cells with the complete medium (DMEM supplemented with 5 mM methionine and 5 mM cysteine) and the pulsed cells were either processed immediately as indicated below (Figure 7) or chased in complete medium for different periods of time as specified in the Figure 8 and the text. In one series of experiments, the glucosidase I and II inhibitor castanospermine (200 μg/mL**)** was added to the cells 1 h prior to and maintained during the metabolic labeling.

In both cases, total cellular lysates were prepared in buffer B (0.5% *N*-dodecyl-β-D-maltoside, 25 mM Tris-HCl, pH 7.4, 140 mM NaCl, 10 mM $CaCl_2$, 0.5 mM phenylmethylsuphonyl fluoride, 5 μg/mL leupeptin, 5 μg/mL soybean trypsin inhibitor, and 10 μg/mL benzamidine) and subjected to sequential immunoprecipitation following a preclearing step using Protein G Sepharose (Amersham Pharmacia). The total pool of receptors was immunoprecipitated using agarose-conjugated anti-myc-antibody (Santa Cruz Biotechnology Inc.) in two consecutive steps, whereas those interacting with calnexin were immunoprecipitated using anti-calnexin antibody (Stressgen) and Protein G Sepharose followed by agarose-conjugated anti-myc-antibody. After the first step, the antigens were eluted with 1% SDS, 25 mM Tris-HCl, pH 7.4, and the eluates diluted 10-fold with buffer C (buffer B in which $CaCl_2$ was replaced with 2 mM EDTA and 2

mM 1,10-phenantroline) prior to the next immunoprecipitation step. The immunopurified receptors were solubilized in Laemmli sample buffer (62.5 mM Tris-HCl, pH 6.8, 2% SDS, 10% glycerol, and 0.001% bromophenol blue), resolved on 10% glycine SDS−PAGE, treated with En^{3}hance (NEN Life Science Products), and exposed to Biomax MR film (Kodak) at −80 °C. The relative intensities of the labeled bands on the autoradiograms were analyzed by densitometric scanning with an Agfa Arcus II laser scanner and the data were quantified using NIH image program, version 1.61, subtracting a local background from each lane. The half-life constants were calculated by fitting the data to a one-phase exponential decay equation using the GraphPad Prism program version 2.01.

Saturation Binding and cAMP Accumulation. Saturation binding isotherms were carried out using [^{3}H] AVP (NEN Life Sciences Products) in the presence or absence of an excess (10^{-5} M) of unlabeled AVP (Peninsula Laboratories) as previously described (*15*). Data for saturation binding experiments were analyzed by nonlinear regression analysis using the ALLFIT program (*34*) for the determination of dissociation constants (k_D) and the total number of receptors (B_{max}).

For cAMP accumulation assays, cells were metabolically labeled with [^{3}H] adenine (NEN Life Sciences Products) for 16 h and total cAMP was purified over Dowex/alumina sequential chromatography as previously described (*35*).

Immunofluorescence and Fluorescence-Assisted Cell Sorting (FACS). Immunofluorescence microscopy was carried out on COS-1 cells that were transiently transfected with the indicated receptors. Cell surface immunofluorescence was performed on viable cells at 4 °C; the cells were incubated with anti-myc antibody (Stressgen), rinsed extensively with DMEM/HEPES, and fixed with 3% paraformaldehyde (PFA) in PBS. Nonspecific sites were quenched with a blocking buffer (PBS containing 0.2% bovine serum albumin) and the cells were incubated with Oregon green-conjugated goat anti-mouse antibody (Molecular Probes) for visualization by microscopy. For intracellular labeling, the cells were first fixed with 3% PFA in PBS and incubated with 0.2% Triton X-100 in PBS. Labeling with anti-myc antibody and Oregon green-conjugated anti-mouse antibody is as described above. Cells were viewed on a Zeiss Axioskop fluorescent microscope (Carl Zeiss Inc.).

For flow cytometry, the cells were washed with PBS and incubated with the 9E10 antibody followed by a second round of washings and incubation with phycoerythrin-conjugated goat anti-mouse IgG (Immunotech). The cells were washed with PBS, fixed with 3% paraformaldehyde, and analyzed on a FACS calibur Becton-Dickson flow cytometer (Becton-Dickson Immunocytometer Systems) set up to detect phycoerythrin fluorescence (585 ± 21 nm); 10 000 cells were analyzed for each sample.

Confocal Microscopy. Intracellular labeling of COS-1 cells expressing the WT or mutant AVPR2 was performed on permeabilized cells as described above except that the cells were incubated with either mouse anti-myc (9E10) antibody (Stressgen), rabbit anti-calreticulin antibody (Stressgen), or rabbit anti-Golgi p58 protein antibody (Sigma). The myc-tagged AVPR2 were revealed with Oregon green-conjugated goat anti-mouse antibody (Molecular Probes) and the ER or Golgi compartments were revealed with Texas-Red-conjugated goat anti-rabbit antibody (Molecular Probes). Double labeling was viewed on a Biorad MRC 600 laser confocal microscope (BioRad Laboratories).

RESULTS

Transcription and Translation of AVPR2 Mutants. The schematic representation of four NDI-causing mutations characterized in this study (S315R, a point mutation in the seventh transmembrane domain; 804delG, a frameshift in the middle of the third intracellular loop; W71X and R337X, two nonsense mutations that code for truncated AVPR2 within the first cytoplasmic loop and the proximal portion of the carboxyl tail, respectively) are shown in Figure 1.

The expression of the transcript for the WT and mutant AVPR2 constructs was assessed in COS-1 cells. In all cases, RT-PCR analyses revealed the presence of RNAs of 1.3 kilobases corresponding to the expected size for the AVPR2 cDNA (Figure 2) indicating that all receptors were actively transcribed.

To determine if the transcripts could be translated into stable proteins, Western blot analyses were carried out using the anti-myc antibody (9E10) that recognizes the myc epitope fused at the N-terminus of each constructs. For the WT receptor, two broad immunoreactive species (41−44 and 72−90 kDa) corresponding to the monomer and dimer forms of the receptor were consistently observed (Figure 3A, lane 2). As expected for a single point mutation, an identical electrophoretic mobility pattern was observed for the S315R mutant receptor (Figure 3A, lane 3). The R337X mutation codes for a truncated receptor that is lacking the last 34 amino acids of the carboxyl tail; therefore, this receptor migrated as smaller species at 34−39 kDa (monomer) and 60−72 kDa (dimer) (Figure 3A, lane 4). Interestingly, an additional band at 97−117 kDa was detected for this mutant. This species could represent a higher order assembly that is visible given the high expression levels obtained for the R337X AVPR2. The 804delG mutant failed to produce any detectable receptor protein and was not tested further (Figure 3A, lane 5). The W71X mutation codes for a truncated AVPR2 that encompasses only the first 71 amino acids. This receptor fragment was separated on tricine SDS−PAGE and detected as a 11.2-kDa protein band (Figure 3B, lane 2). To demonstrate that this band is not a degradation product of the full length AVPR2, the WT receptor was migrated as a control and did not lead to the detection of an equivalent immunoreactive species (Figure 3B, lane 1).

Pharmacological and Functional Characterization of AVPR2 Mutants. To investigate the pharmacological properties of the expressed mutant receptors, whole-cell saturation binding assays were carried out using [^{3}H]AVP as the radioligand in the presence and absence of excess (10 μM) unlabeled AVP to define nonspecific binding (Figure 4A). The WT receptor was expressed at 1.3 pmol/well and displayed an affinity of 2.7 nM for AVP. In contrast, no specific binding to [^{3}H]AVP could be detected for any of the AVPR2 mutants tested.

In agreement with the lack of AVP binding, none of the mutant AVPR2 expressed conferred an AVP-sensitive adenylyl cyclase activity to the transfected COS-1 cells. This contrasts with the AVP-stimulated cAMP production observed in COS-1 cells expressing the WT AVPR2 (Figure 4B).

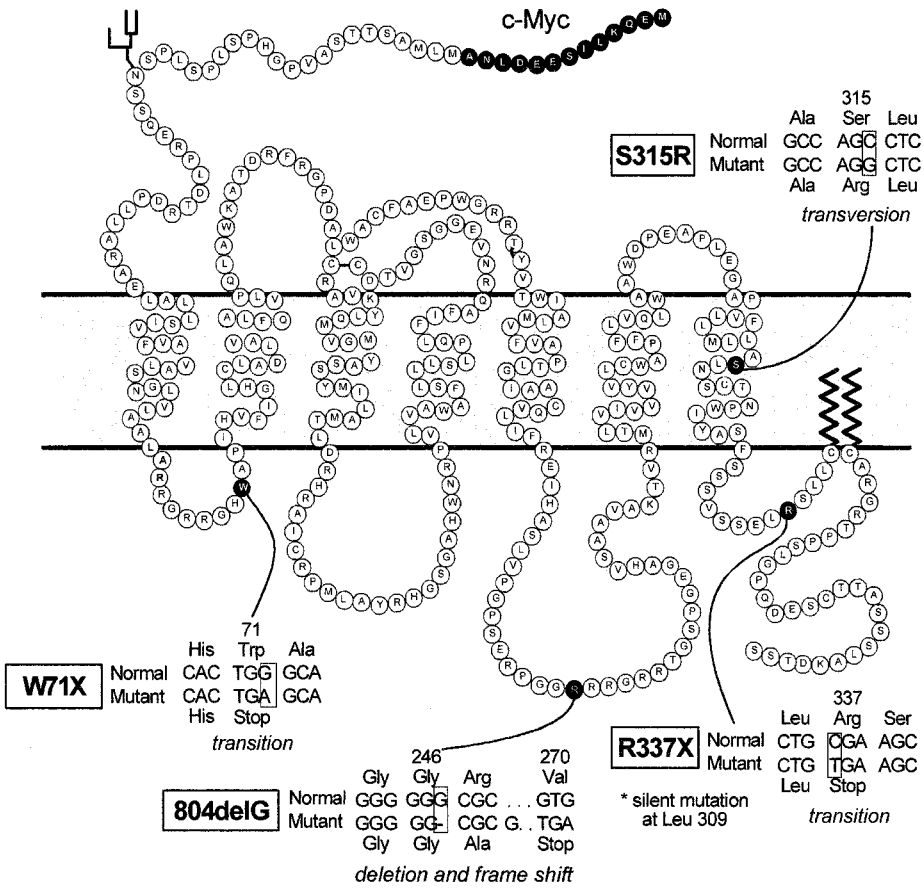

FIGURE 1: Schematic representation of the AVPR2 showing the nature and position of four mutations causing NDI. The seven transmembrane schematic of the AVPR2 is depicted with an extracellular amino-terminus bearing a c-myc epitope tag, a N-linked oligosaccharide at N22, a disulfide bridge between C112 and C192, and the two palmitoylated cysteines (C341 and C342). Mutations are described by indicating the amino acid position and the specific nucleotide change.

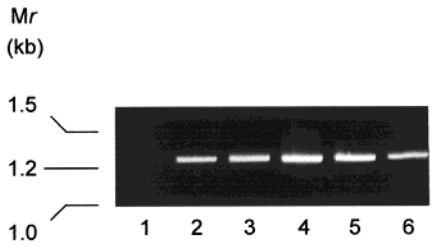

FIGURE 2: RNA transcription of the wild type and mutant AVPR2. COS-1 cells were transfected with WT or mutant AVPR2, the total RNA was isolated and cDNA prepared by reverse transcription and PCR as described in Experimental Procedures. cDNAs were then revealed by ethidium bromide labeling following migration on a 0.8% agarose gel. Lane 1: vector; 2: WT; 3: W71X; 4: 804delG; 5: R337X; and 6: S315R AVPR2.

Absence of Cell-Surface Targeting of AVPR2 Mutants. To determine whether the lack of binding activity resulted from mistargeting of mutant proteins, immunofluorescence studies were carried out in intact and permeabilized COS-1 cells. Whereas the WT and S315R AVPR2 could be detected on the surface of nonpermeabilized cells, no signal was observed for the W71X and R337X mutant receptors (Figure 5A). When cells were permeabilized, all receptors were detected intracellularly (Figure 5C) indicating that, in all cases, proteins were synthesized and accumulated in cells but that the R337X and W71X were not properly targeted to the plasma membrane. FACS analysis confirmed the lack of cell surface expression for W71X and R337X AVPR2 and indicated that S315R was targeted to the cell surface (Figure 5D).

ER−Retention of Mutant AVPR2. The subcellular distribution of the wild type and each of the mutant receptors was determined using confocal microscopy. The 9E10 antibody was used to detect the myc-tagged AVPR2 receptors, while the anti-calreticulin and anti-p58 antibodies were used to label the ER and Golgi compartments, respectively. Both the WT and S315R AVPR2 colocalized with the ER and Golgi markers indicating that they could enter the secretory pathway and be properly processed (Figure 6A−F and S−X, respectively). This is consistent with the cell surface expression detected in Figure 5. In contrast, the W71X and R337X could only be detected in the ER (Figure 6G−L and M−R, respectively) indicating that they were retained by the quality control system and could never reach the Golgi apparatus in agreement with their lack of cell surface expression (Figure 5).

Molecular Association of the AVPR2 with Calnexin. To investigate whether the molecular chaperone calnexin can interact with the AVPR2, co-immunoprecipitation experiments were carried out. For this purpose, transiently transfected COS-1 cells expressing either the WT or the mutant receptors were metabolically labeled with [^{35}S]-methionine/cysteine. The presence of the myc-tagged AVPR2 in the fraction immunoprecipitated with the anti-calnexin antibody was assessed by a second immunoprecipitation using agarose-conjugated 9E10 antibody. The WT, S315R, and R337X,

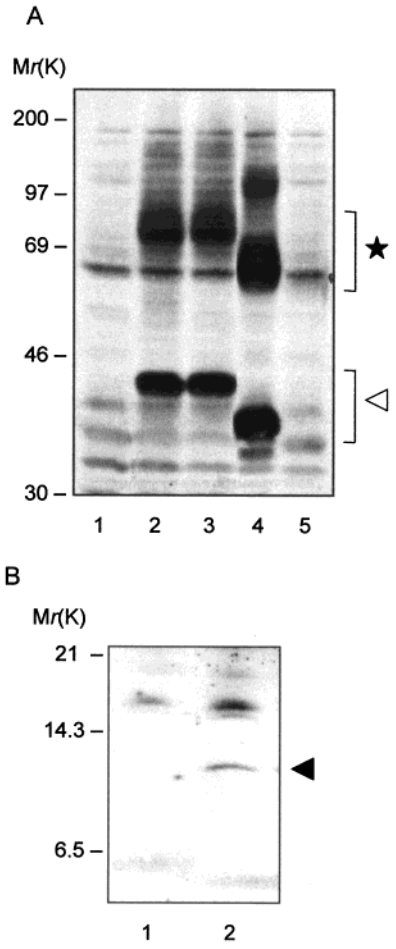

FIGURE 3: Western blot analysis of the wild type and mutant AVPR2. COS-1 cells were transfected with WT or mutant AVPR2 and the proteins from crude membrane preparations were separated on 10% SDS−PAGE (A) or 16.5% Tricine SDS−PAGE (B) (100 μg of total protein per lane), transferred onto nitrocellulose filters, incubated with 9E10 monoclonal antibody followed by HRP-conjugated sheep anti-mouse F(ab′)$_2$ fragment. (A) Lane 1: vector; 2: WT; 3: S315R; 4: R337X; and 5: 804delG AVPR2. The position of the AVPR2 monomers and dimers are denoted by an arrowhead and an asterisk, respectively. (B) Protein expression of the W71X receptor. Lane 1: WT and 2: W71X AVPR2. The position of the W71X AVPR2 is indicated by an arrowhead. All protein bands were revealed by chemiluminescence.

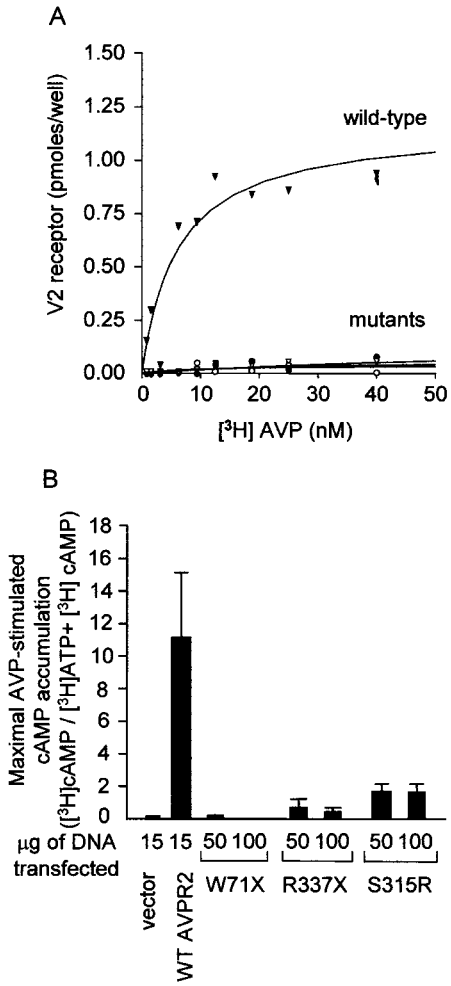

FIGURE 4: Binding and signaling activities of the wild type and mutant AVPR2. COS-1 cells were transfected with the wild type (▼) or mutant AVPR2; R337X (●), S315R (▽), or W71X (○). (A) Cells were incubated with varying concentrations of [^{3}H] AVP in the presence and absence of 10 μM unlabeled AVP. Specific binding (shown in pmoles/well) was determined by subtracting total from nonspecific binding. (B) cAMP accumulation in cells expressing the WT and mutant AVPR2. The amount of DNA transfected for each construct is indicated. cAMP accumulation was expressed as the difference in cAMP production between AVP-stimulated (10 μM) and unstimulated cells presented as the ratio of cAMP over ATP + cAMP.

but not the W71X (data not shown) mutant AVPR2 co-immunoprecipitated with calnexin (Figure 7). The specificity of this interaction was confirmed by the observation that no receptors were detected when the first immunoprecipitation was carried out with preimmune serum. Although coimmunprecipitation is often used to document calnexin−substrate interactions, one cannot exclude the possibility that indirect interaction involving additional proteins could be involved. However, the observation that only the precursor and not the mature form of the receptor was found associated with calnexin, rules out the possibility of a large nonspecific aggregation and is consistent with the role of calnexin as an ER chaperone. To further document if the interaction between calnexin and vasopressin resulted from the chaperoning role of the former, the effect of the glucosidase I and II inhibitor castanospermine was assessed on the extent of the interaction. As shown in Figure 7B, castanospermine drastically reduced the association of calnexin with the newly synthesized AVPR2, confirming that the interaction results from the quality control activity of calnexin.

For a number of misfolded proteins, a prolonged association with calnexin has been proposed to play an important role in their ER retention (see Introduction). To determine if calnexin could play such a role in retaining NDI-causing AVPR2 mutations, the interaction between calnexin and the ER-retained R337X mutant was investigated further. For this purpose, HEK-293 cells stably expressing either the WT or the R337X AVPR2 were metabolically labeled with [^{35}S] methionine/cysteine and chased for the indicated periods of time (Figure 8A−D). For each time point, the proportion of receptors associated with calnexin was assessed using sequential immunoprecipitation with anti-calnexin and 9E10 antibodies as described above. In parallel samples, the total population of receptors was directly immunoprecipitated using only the 9E10 antibody. Direct immunoprecipitation of the receptor allowed a visualization of both the precursor (29−33 kDa) and mature (40−42 kDa) forms of the receptor

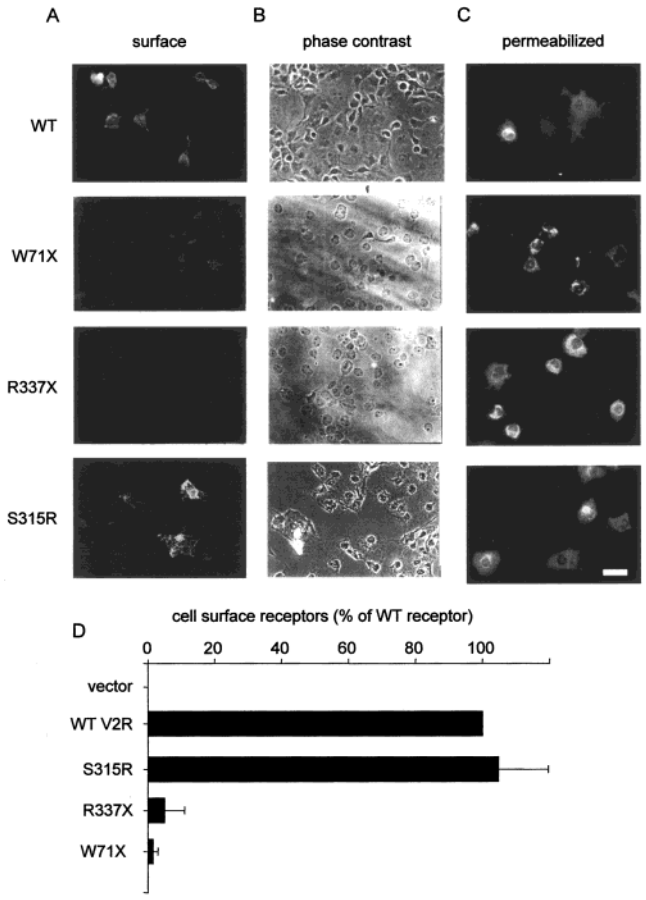

FIGURE 5: Cell surface expression of WT and mutant AVPR2. Transfected COS-1 cells were incubated in the absence (A) or presence (C) of 0.2% Triton X-100 in PBS. The cells were then incubated with the 9E10 monoclonal antibody followed by Oregon green-conjugated donkey anti-mouse antibody. (B) The same field of cells shown in panel A, viewed by phase contrast microscopy. Bar equals 50 μm. (D) Quantification of cell surface WT and mutant AVPR2 by FACS. The cells were incubated with 9E10 antibody followed by phycoerythrin-conjugated goat anti-mouse antibody. For each sample, 10 000 cells were analyzed. The values were calculated by multiplying the fluorescence intensity by the number of positive cells detected for each receptor constructs and normalized to the signals obtained with cells transfected with the empty vector (0%) and the WT AVP2R construct (100%).

(Figure 8B). For the WT AVPR2, the precursor disappears rapidly ($t_{1/2}$ of 50 min) at the expense of the mature form of the receptor. This contrasts with the inefficient maturation of the R337X mutant for which almost no mature form could be detected (Figure 8D). Consistent with the ER retention profile reported in Figure 6, the half-life of the R337X precursor form was found to be approximately twice as long ($t_{1/2}$ of 98 min) as that of the WT AVPR2 precursor. For both the WT and R337X AVPR2, only the precursor forms could be coimmunoprecipitated with calnexin (Figure 8A and C). In an effort to quantify the association time between the receptor and calnexin, the ratio between the calnexin-associated receptor and the total amount of immunoprecipitated receptor precursor was calculated for each chase time point. The proportion of precursor form associated with calnexin was greater for R337X than for the WT AVPR2 for each chase time point considered, indicative of a lower dissociation rate between the mutant receptor and the molecular chaperone (Figure 8E). When the S315R AVPR2 mutant that can reach the cell surface but does not bind vasopressin was considered, an association pattern intermediate between that of the WT and R337X was obtained.

DISCUSSION

In this study, we have characterized the biosynthesis, subcellular distribution, and function of four NDI-mutant AVPR2. When expressed in heterologous systems, three of the four receptor genes produced identifiable proteins as assessed by Western blotting. The only AVPR2 that was not synthesized is the 804delG mutant. This may not be surprising since another mutation occurring in this guanine-rich region, the insertion of a guanine nucleotide at position 804 (804insG), was also found to produce no protein despite adequate mRNA levels (*11*). It therefore appears that the addition or removal of a single guanine residue in this region of the *avpr2* gene disrupts normal protein synthesis or greatly impair protein stability. The mechanism underlying this phenomenon remains to be investigated.

For the W71X and R337X AVPR2 mutants, we observed intracellular retention of the synthesized protein with very little or no cell surface routing. The lack of cell surface expression of the W71X mutant most likely does not result from the lack of translocation since our results show that it accumulates in the ER. This is consistent with a previous report demonstrating that this mutant is synthesized and properly oriented in *Escherichia coli* (*6*). However, the lack of cell surface expression observed in the present study differs from previous findings on a fusion protein between W71X and the carboxyl terminus of the WT AVPR2 that was fused to green fluorescent protein (GFP) where this construct was detected at the surface of transfected HEK 293 cells (*20*). A possible explanation for this apparent contradiction is that a GFP moiety may stabilize the W71X mutant and allow it to be targeted to the cell surface.

Intracellular retention of the R337X mutation is consistent with previous studies (*7*, *14*, *17*). However, here we report for the first time that this receptor is retained in the ER and never reaches the Golgi compartment indicating that misfolding provoked by the mutation does not allow the receptor protein to escape the ER quality control system.

Our study has also allowed us to uncover a mutation (S315R) that, although targeted to the cell surface, is unable to bind AVP and to generate an intracellular signal. Although several mutations lead to compromise AVP binding in most cases this results from lack of cell surface expression of the receptor. In the few cases where binding deficient mutant receptors were targeted to the cell surface, a decrease in the affinity for AVP rather than a total loss of binding has generally been observed (*4*, *8*, *9*, *12*, *16*, *25*, *36*). Besides S315R, the only other mutations for which total loss of detectable binding were reported are W99R (*18*), R202C, and G185C (*52*). Similar to what was observed for S315R, lack of radioligand binding for these three mutants occurred despite a significant trafficking of the receptor at the cell surface. However, in contrast with S315R and G185C, a significant AVP-mediated cAMP response was observed in cells expressing W99R and R202C indicating that although not detected with the radioligands, these two mutants maintained some AVP binding ability. S315R and G185C thus represent the first examples of "binding-null" mutants that are expressed at the cell surface.

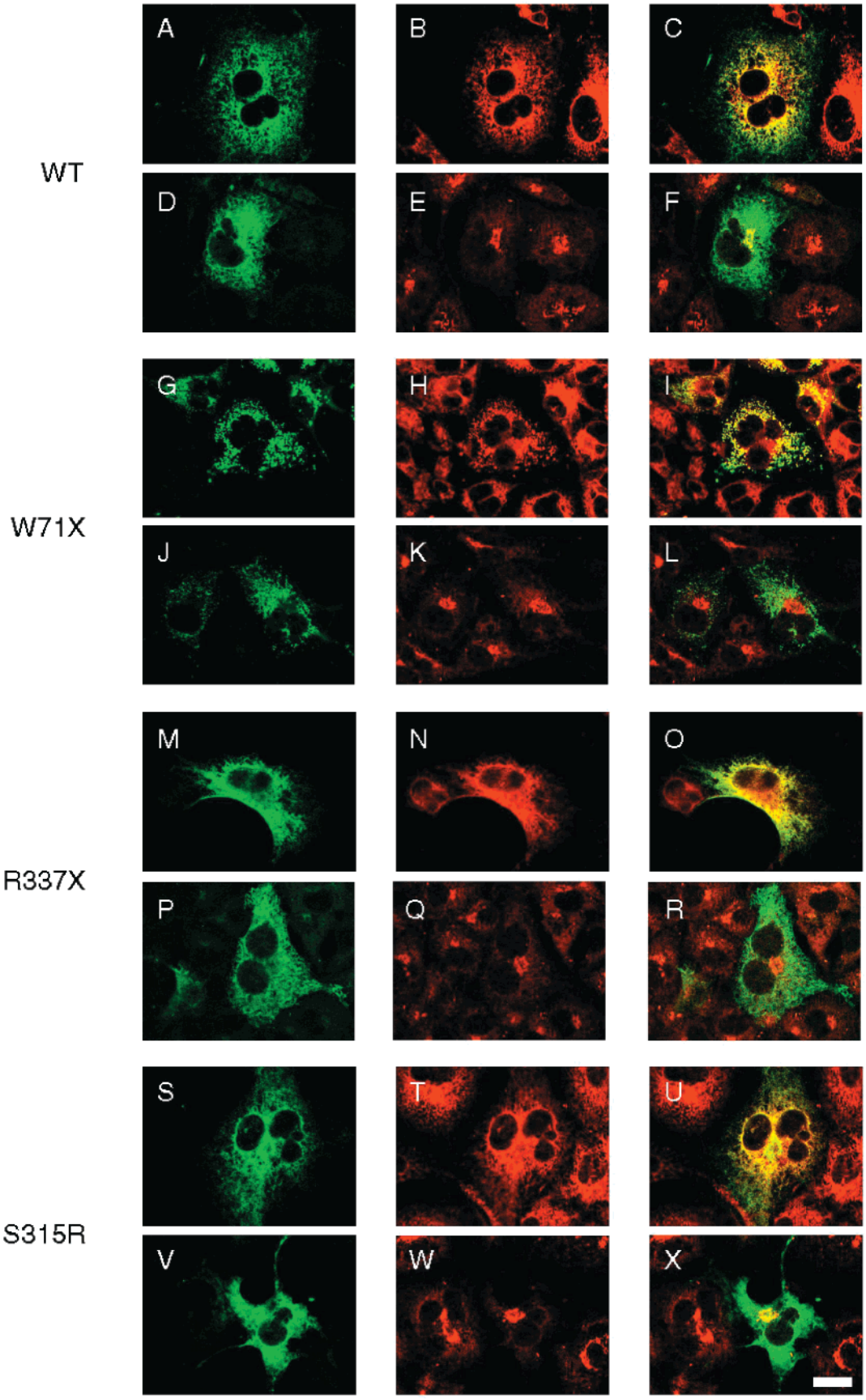

FIGURE 6: Intracellular distribution of WT and mutant AVPR2. COS-1 cells were transiently transfected with the indicated AVPR2 constructs and permeabilized to visualize intracellular receptors (left panels) and the ER or Golgi markers (middle panels). Immunoreactivity of WT and mutant receptors was detected using the anti-myc antibody recognizing the N-terminus epitope added to the receptors (A, D, G, J, M, P, S, and V). The same fields of cells were stained with anti-calreticulin antibody to visualize the ER (B, H, N, and T) or with anti-p58 antibody to visualize the Golgi apparatus (E, K, Q, and W). The right panels show the merged images of the receptor and ER labeling (C, I, O, and U) or of the receptor with the Golgi apparatus (F, L, R, and X). Bar equals 20 μm.

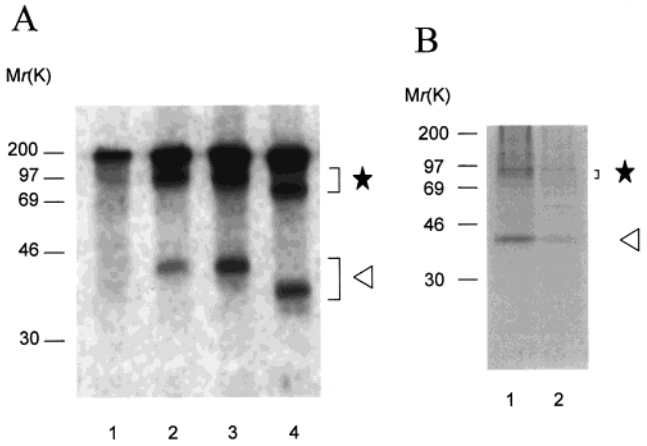

FIGURE 7: Association of mutant AVPR2 with the molecular chaperone calnexin. Metabolic labeling of the WT and mutant AVPR2 expressed in COS-1 cells was carried out with [^{35}S] methionine/cysteine and sequential immunoprecipitations were performed on cell lysates using anti-calnexin antibody and Protein G-Sepharose followed by agarose conjugated anti-myc antibody. (A) The labeling was carried out in cells expressing: vector (lane 1), WT (lane 2), S315R (lane 3), and R337X (lane 4) AVPR2. (B) The labeling was carried out in cells expressing the WT AVPR2 treated (lane 2) or not (lane 1) with castanospermine. The position of the AVPR2 monomers and dimers is denoted by an arrowhead and an asterisk, respectively.

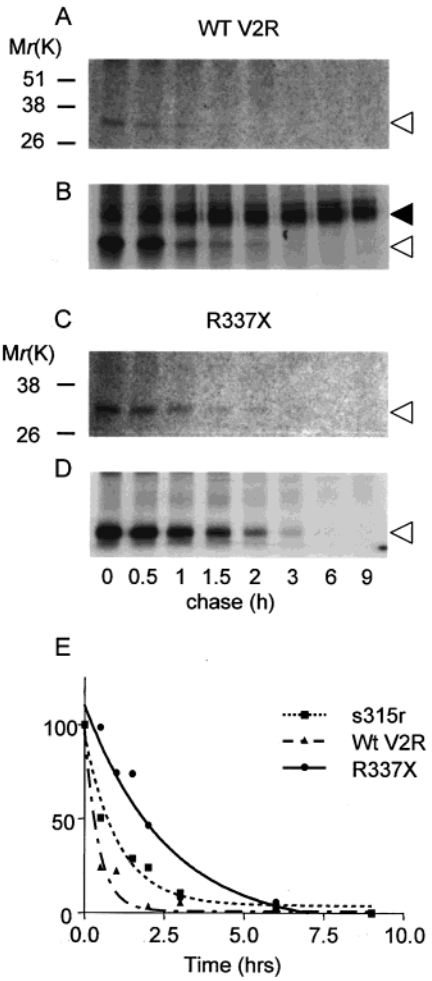

FIGURE 8: Prolonged association of the R337X mutant AVPR2 with calnexin during biogenesis. Metabolic labeling of the WT and R337X AVPR2 stably expressed in HEK-293 cells was carried out as described in Experimental Procedures. Cells expressing the WT (A and B) and R337X (C and D) AVPR2 were labeled for 30 min and chased for the indicated times. Sequential immunoprecipitations were carried out with anti-calnexin antibody and Protein G-Sepharose followed by agarose-conjugated anti-myc antibody (panels A and C) or two repetitions of the agarose-conjugated anti-myc antibody (panels B and D). Precursor and mature forms of the receptors are indicated by opened and closed arrowheads, respectively. (E) Graphical representation of the interaction kinetics for the WT, R337X, and S315R AVPR2 with calnexin. Densitometric analysis of the total receptor precursors (B and D, open arrowheads) and calnexin-interacting receptors (A and C, open arrowheads) were carried out for each chase time. The extent of calnexin association was determined at each chase time by dividing the signal obtained for the precursor coimmunoprecipitated with calnexin by the total amount of precursor. A value of 100% was assigned to the ratio determined at the 0 min time point for each receptor construct. The half-life of the calnexin interaction with the WT, R337X and S315R AVPR2 was found to be 20, 107, and 44 min, respectively, as determined by fitting the data to a one-phase exponential decay equation.

Although the molecular mechanisms involved in quality control are not fully understood, several studies suggest that interaction of sugar moieties and/or exposed hydrophobic patches in misfolded proteins with molecular chaperones plays an important role in this process. This has been well characterized for a number of proteins (*26*, *37*, *38*); however, very little is known on the quality control criteria for the folding of GPCRs. To date, only a few studies have reported molecular chaperone interactions with GPCRs. RanBP2 and nina A, two cyclophilin-related proteins, were shown to act as molecular chaperones for the red/green opsin (*39*) and rhodopsin (*40*, *41*), respectively, whereas calnexin was found to associate with the receptor for lutropin/choriogonadotropin (LHR) and follitropin (FSHR) (*31*). Calnexin interacts with monoglucosylated *N*-linked carbohydrate chains (*42*) and peptide determinants (*43*) on folding intermediates of target proteins. Like for the LH and FSH receptors, WT AVPR2 was found to interact with calnexin. In addition, both cell surface targeted and ER-retained mutant receptors could also associate with this molecular chaperone in agreement with its general role in protein folding. Consistent with this role, detailed analysis of the molecular species interacting with calnexin demonstrated that it is the precursor, and not the fully processed form of the receptor, that binds to this chaperone. Also, castanospermine inhibited the association of the AVPR2 with calnexin. Given that this compound prevents the generation of the monoglucosylated forms of protein precursor that are the synthesis intermediate bound by calexin, it confirms that the interaction with calnexin does occur during the receptor maturation process.

The fact that calnexin associates for a longer period of time with the ER-retained R337X mutant than with the WT AVPR2 suggests that in addition to its role in assisting the folding of GPCRs, this chaperone could also be involved in the retention of inappropriately folded receptors. Such a role for calnexin in quality control has previously been proposed for the cystic fibrosis transmembrane conductance regulator (*29*, *30*), the melanin-synthesizing enzyme, tyrosinase (*28*), and the multidrug-resistance gene product, P-glycoprotein (*27*). Interestingly, the mutant S315R that can reach the cell surface was also found to have a slightly prolonged interaction with calnexin when compared to the WT (a half time of association of 44 vs 20 min) but much shorter than that of R337X (107 min). This indicates that even mutant receptors that become trafficking competent may interact for

extended periods with the molecular chaperone, maybe reflecting the need for a longer folding time. This is entirely consistent with the dual role proposed for calnexin (*26*). On one hand, the chaperone is believed to assist folding of neosynthesized proteins, while on the other hand it targets the incompletely or misfolded proteins toward the degradation pathway. According to the current models, proteins that cannot reach a conformation that is compatible with ER export within a given period of time would be retrotranslocated in the cytosol and targeted to the proteasome for degradation. The nature of the molecular sensor and biological clock determining how long a protein is retained in the ER before it is either exported to the cell surface or targeted for degradation remains unknown. Nevertheless, R337X and S315R clearly exemplify the distinct fate of mutant proteins.

Subtle protein misfolding leading to the ER retention of otherwise functional proteins is at the root of several human diseases (for a review, see ref *44*). A better understanding of the molecular mechanisms involved in the quality control system could lead to new therapeutic avenues for these diseases. In previous studies, treatments with both selective (*15*, *45*−*47*) and nonselective agents (*48*−*51*) termed pharmacological and chemical chaperones, respectively, were found to favor the escape of mutant, misfolded proteins from the ER quality control system. Treatment with pharmacological chaperones was found to rescue the cell surface targeting and function of several AVPR2 mutations responsible for NDI (*15*). Whether these agents act by modifying the kinetics of interaction between calnexin and the mutant AVPR2 remains to be investigated.

ACKNOWLEDGMENT

We thank L. Cournoyer and Mireille Hogue for technical assistance, M. Moreau for assistance with the figures, S. Sénéchal for FACS analysis, and Dr. L. Rokeach for critical reading of the manuscript.

REFERENCES

1. Birnbaumer, M., Seibold, A., Gilbert, S., Ishido, M., Barberis, C., Antaramian, A., Brabet, P., and Rosenthal, W. (1992) *Nature 357*, 333−5.
2. Fushimi, K., Uchida, S., Hara, Y., Hirata, Y., Marumo, F., and Sasaki, S. (1993) *Nature 361*, 549−52.
3. Bichet, D., and Fujiwara, T. (2000) in *The Metabolic and Molecular Bases of Inherited Disease* (Scriver, C., Beaudet, A., Sly, W., Vallee, D., Childs, B., and Vogelstein, B., Eds.) McGraw-Hill, New York, in press.
4. Oksche, A., Schulein, R., Rutz, C., Liebenhoff, U., Dickson, J., Muller, H., Birnbaumer, M., and Rosenthal, W. (1996) *Mol. Pharmacol. 50*, 820−8.
5. Ala, Y., Morin, D., Mouillac, B., Sabatier, N., Vargas, R., Cotte, N., Dechaux, M., Antignac, C., Arthus, M. F., Lonergan, M., Turner, M. S., Balestre, M. N., Alonso, G., Hibert, M., Barberis, C., Hendy, G. N., Bichet, D. G., and Jard, S. (1998) *J. Am. Soc. Nephrol. 9*, 1861−72.
6. Schulein, R., Rutz, C., and Rosenthal, W. (1996) *J. Biol. Chem. 271*, 28844−52.
7. Sadeghi, H. M., Innamorati, G., and Birnbaumer, M. (1997) *Mol. Endocrinol. 11*, 706−13.
8. Birnbaumer, M., Gilbert, S., and Rosenthal, W. (1994) *Mol. Endocrinol. 8*, 886−94.
9. Pan, Y., Wilson, P., and Gitschier, J. (1994) *J. Biol. Chem. 269*, 31933−7.
10. Rosenthal, W., Antaramian, A., Gilbert, S., and Birnbaumer, M. (1993) *J. Biol. Chem. 268*, 13030−3.
11. Tsukaguchi, H., Matsubara, H., Taketani, S., Mori, Y., Seido, T., and Inada, M. (1995) *J. Clin. Invest. 96*, 2043−50.
12. Yokoyama, K., Yamauchi, A., Izumi, M., Itoh, T., Ando, A., Imai, E., Kamada, T., and Ueda, N. (1996) *J. Am. Soc. Nephrol. 7*, 410−4.
13. Schoneberg, T., Yun, J., Wenkert, D., and Wess, J. (1996) *EMBO J. 15*, 1283−91.
14. Wenkert, D., Schoneberg, T., Merendino, J. J., Jr., Rodriguez Pena, M. S., Vinitsky, R., Goldsmith, P. K., Wess, J., and Spiegel, A. M. (1996) *Mol. Cell Endocrinol. 124*, 43−50.
15. Morello, J. P., Salahpour, A., Laperriere, A., Bernier, V., Arthus, M. F., Lonergan, M., Petaja-Repo, U., Angers, S., Morin, D., Bichet, D. G., and Bouvier, M. (2000) *J. Clin. Invest. 105*, 887−95.
16. Pasel, K., Schulz, A., Timmermann, K., Linnemann, K., Hoeltzenbein, M., Jaaskelainen, J., Gruters, A., Filler, G., and Schoneberg, T. (2000) *J. Clin. Endocrinol. Metab. 85*, 1703−10.
17. Oksche, A., Dehe, M., Schulein, R., Wiesner, B., and Rosenthal, W. (1998) *FEBS Lett. 424*, 57−62.
18. Albertazzi, E., Zanchetta, D., Barbier, P., Faranda, S., Frattini, A., Vezzoni, P., Procaccio, M., Bettinelli, A., Guzzi, F., Parenti, M., and Chini, B. (2000) *J. Am. Soc. Nephrol. 11*, 1033−43.
19. Innamorati, G., Sadeghi, H., and Birnbaumer, M. (1996) *Mol. Pharmacol. 50*, 467−73.
20. Krause, G., Hermosilla, R., Oksche, A., Rutz, C., Rosenthal, W., and Schulein, R. (2000) *Mol. Pharmacol. 57*, 232−42.
21. Zhu, X., and Wess, J. (1998) *Biochemistry 37*, 15773−84.
22. Morin, D., Cotte, N., Balestre, M. N., Mouillac, B., Manning, M., Breton, C., and Barberis, C. (1998) *FEBS Lett. 441*, 470−5.
23. Schulein, R., Hermosilla, R., Oksche, A., Dehe, M., Wiesner, B., Krause, G., and Rosenthal, W. (1998) *Mol. Pharmacol. 54*, 525−35.
24. Innamorati, G., Sadeghi, H., Eberle, A. N., and Birnbaumer, M. (1997) *J. Biol. Chem. 272*, 2486−92.
25. Postina, R., Ufer, E., Pfeiffer, R., Knoers, N. V., and Fahrenholz, F. (2000) *Mol. Cell. Endocrinol. 164*, 31−9.
26. Bross, P., Corydon, T. J., Andresen, B. S., Jorgensen, M. M., Bolund, L., and Gregersen, N. (1999) *Hum. Mutat. 14*, 186−98.
27. Loo, T. W., and Clarke, D. M. (1994) *J. Biol. Chem. 269*, 28683−9.
28. Halaban, R., Svedine, S., Cheng, E., Smicun, Y., Aron, R., and Hebert, D. N. (2000) *Proc. Natl. Acad. Sci. U.S.A. 97*, 5889−94.
29. Pind, S., Riordan, J. R., and Williams, D. B. (1994) *J. Biol. Chem. 269*, 12784−8.
30. Yang, Y., Janich, S., Cohn, J. A., and Wilson, J. M. (1993) *Proc. Natl. Acad. Sci. U.S.A. 90*, 9480−4.
31. Rozell, T. G., Davis, D. P., Chai, Y., and Segaloff, D. L. (1998) *Endocrinology 139*, 1588−93.
32. Cullen, B. R. (1987) *Methods Enzymol. 152*, 684−704.
33. Schagger, H., and von Jagow, G. (1987) *Anal. Biochem. 166*, 368−79.
34. DeLean, A., Munson, P. J., and Rodbard, D. (1978) *Am. J. Physiol. 235*, E97−102.
35. Wong, Y. H., Federman, A., Pace, A. M., Zachary, I., Evans, T., Pouyssegur, J., and Bourne, H. R. (1991) *Nature 351*, 63−5.
36. Sadeghi, H., Robertson, G. L., Bichet, D. G., Innamorati, G., and Birnbaumer, M. (1997) *Mol. Endocrinol. 11*, 1806−13.
37. Kim, P. S., and Arvan, P. (1998) *Endocr. Rev. 19*, 173−202.
38. Kuznetsov, G., and Nigam, S. K. (1998) *N. Engl. J. Med. 339*, 1688−95.
39. Ferreira, P. A., Nakayama, T. A., Pak, W. L., and Travis, G. H. (1996) *Nature 383*, 637−40.
40. Colley, N. J., Baker, E. K., Stamnes, M. A., and Zuker, C. S. (1991) *Cell 67*, 255−63.

41. Baker, E. K., Colley, N. J., and Zuker, C. S. (1994) *EMBO J. 13*, 4886−95.
42. Ou, W. J., Cameron, P. H., Thomas, D. Y., and Bergeron, J. J. (1993) *Nature 364*, 771−6.
43. Ihara, Y., Cohen-Doyle, M. F., Saito, Y., and Williams, D. B. (1999) *Mol. Cell 4*, 331−41.
44. Morello, J. P., Petaja-Repo, U. E., Bichet, D. G., and Bouvier, M. (2000) *Trends Pharmacol. Sci. 21*, 466−469.
45. Fan, J. Q., Ishii, S., Asano, N., and Suzuki, Y. (1999) *Nat. Med. 5*, 112−5.
46. Foster, B. A., Coffey, H. A., Morin, M. J., and Rastinejad, F. (1999) *Science 286*, 2507−10.
47. Loo, T. W., and Clarke, D. M. (1997) *J. Biol. Chem. 272*, 709−12.
48. Brown, C. R., Hong-Brown, L. Q., Biwersi, J., Verkman, A. S., and Welch, W. J. (1996) *Cell Stress Chaperones 1*, 117−25.
49. Sato, S., Ward, C. L., Krouse, M. E., Wine, J. J., and Kopito, R. R. (1996) *J. Biol. Chem. 271*, 635−8.
50. Burrows, J. A., Willis, L. K., and Perlmutter, D. H. (2000) *Proc. Natl. Acad. Sci. U.S.A. 97*, 1796−801.
51. Tamarappoo, B. K., Yang, B., and Verkman, A. S. (1999) *J. Biol. Chem. 274*, 34825−31.
52. Schulein, R., Zuhlke, K., Okshe, A., Hermosilla, R., Furkert, J. and Rosenthal, W. (2000) *FEBS Lett. 473*, 124−127.

BI002699R